Hybrid wind-wave systems: The case of the VolturnUS-S semi-submersible platform

Maximilian Hengstmann, Juan C. C. Portillo, and Luís M. C. Gato

Abstract—**Wind-wave hybrid floating systems are subject to active research and development in academia and industry. Industrialization of hybrid wind-wave energy systems will benefit from modular designs, allowing floating platforms to be used with or without wave energy converters (WECs). This work explores the design process to use oscillating water column (OWC) WECs as modular add-on features to existing semi-submersible floating platform designs. As the base case design, the IEA 15 MW offshore reference wind turbine with the VolturnUS-S floating platform designed by the University of Maine was used. The proposed decoupled simulation procedure involved OpenFAST developed by NREL and the OWC Modelica tool developed at IST/ULisboa. Aero-hydro-servo-elastic simulations were performed to analyze the influence of the wind turbine energy generation design modifications and damage equivalent loads (DELs). The hybrid platform was modeled in the OWC Modelica tool to assess the wave energy conversion and the interaction between OWCs and the floating platform. The investigated hybrid design did not significantly increase DELs of the wind turbine in aero-hydro-servo-elastic simulations. The hybrid system does not decrease the LCOE compared to a standalone floating wind turbine due to high CAPEX and low energy yield. Furthermore, the coupling forces between OWCs and the floating platform were found to be in the same order of magnitude as the wave excitation and radiation forces. This challenges the findings obtained with the decoupled approach used in this paper. The possibilities of including these forces in OpenFAST and the challenges for this are discussed.**

Index Terms—**Hybrid wind-wave device, Floating platform, Wave energy converter, Oscillating water column.**

I. Introduction

THE European Commission set the goals to reduce greenhouse gas emissions by 55% compared to 1990 by 2030 and to become carbon neutral by 2050 [1]. Offshore renewable energy technologies are supposed to play an important role in this transition. According to European Union (EU) goals, offshore wind capacities shall reach 300 GW by 2050, complemented with 40 GW from floating wind and other forms of ocean energy [2].

Floating wind and wave energy currently have a higher levelised cost of electricity (LCOE) than the renewable energies widely used for power generation today [3], [4]. Accommodating devices on floating platforms poses additional challenges and higher costs than bottom-fixed solutions. Mooring systems, floaters, installation, grid connection, operation, and maintenance represent a high share of the project costs [5]. Grouping multiple energy converters on floating foundations is a potential approach to reduce overall LCOE since costs for many subsystems would then be shared. Further synergy potential lies in the dynamic interaction. In some cases, wave energy converters can act as motion dampers to reduce platform movement and loads on the wind turbine [6]. But research does not allow for general conclusions on this. Instead, results seem to depend on the specific design strongly. Another synergy is reduced intermittency of the combined power output [7]. In light of these advantages, Wind-Wave-Hybrid devices are actively investigated in scientific and industrial environments [8]–[14].

Even though some systems are on their way to commercialization, [15], [16], most wind-wave hybrid concepts only exist as preliminary studies. The hybrid floating system presented in Ref. [15], developed for commercialization, considers a hybrid system. The optimization of coupled hybrid wind-wave systems is a complex process yet to be fully understood, requiring more research, development and innovation. The floating platform and wave energy converters are usually designed and optimised for specific sea states. A modular approach consisting of a standalone platform that can be used by itself and a wave energy converter that can be added if the wave climate is suitable, as presented in Ref. [16], might be an interesting approach towards wide-spreading of wave energy systems, aiding in achieving scale effects and the associated reductions in costs [17]. A general generic approach to include wave energy converters as add-ons to existing floating wind platforms could simplify the development process and increase the number of platforms this solution is pursued for.

Most of the concepts investigated so far include oscillating body wave energy converters [18]. This type of wave energy converter typically requires complex power take-off systems that, in many cases, are submerged in the seawater and therefore suffer from low reliability and a high maintenance demand [19]. A different type of wave energy converter is the oscillating

Sponsor and financial support acknowledgement: This work was supported by the Portuguese Foundation for Science and Technology (FCT) through IDMEC, under LAETA, project UIDB/50022/2020.

M. Hengstmann is studying aerospace engineering at the University of Stuttgart Keplertraße 7, Stuttgart 70174 Germany (e-mail: st117703@stud.uni-stuttgart.de). The first author thanks IDMEC, Instituto Superior Técnico, University of Lisbon (IST/ULisboa), and University of Stuttgart's chair of Wind Energy for the support during the short research visit at IST/ULisboa for developing this work.

J. C. C. Portillo (e-mail: juan.portillo@tecnico.ulisboa.pt) and L. M. C. Gato (e-mail: luis.gato@tecnico.ulisboa.pt) are with IDMEC, Instituto Superior Técnico, Universidade de Lisboa, Av. Rovisco Pais 1, 1049-001 Lisbon, Portugal.

Digital Object Identifier:
https://doi.org/10.36688/ewtec-2023-395

water column (OWC), in which the only moving part is the air turbine, not in contact with the seawater. The reduced complexity of this kind of solution could improve reliability and costs for the wave energy converter (WEC) itself [20] and also for a hybrid system.

This work investigates the process of extending an existing floating wind platform design using OWC wave energy converters as add-on features. A design process is presented and applied to a case study. The basis for the hybrid designs analyzed in this work is the VolturnUS-S semi-submersible floating platform, developed by the University of Maine, supporting the 15 MW IEA reference offshore turbine. The aim of the design process is to i) demonstrate the feasibility of designing OWCs as add-on features to existing wind floating platform designs, ii) keep the loads on the wind turbine close or lower to those of the original design, iii) minimize the levelised cost of electricity (LCOE). To investigate these effects a decoupled simulation approach for the OWCs and the floating wind platform is applied and its validity for the application here is analyzed.

II. Methodology

One of the study's considerations is that the wind turbine's power production shall not be reduced, and the fatigue loads of the floating wind turbine shall not be increased. The other considerations are that the generated power for the OWCs shall be as large as possible, and the additional costs for the added geometry and OWC components be the least.

The addition of OWCs, as they are modeled in this work, changes the floater dynamics in the following ways:

1) Change of the platform mass properties.
2) Change of the geometry and, therefore, the hydrodynamic coefficients.
3) Coupling force due to the pressure variation in the OWC chamber.
4) Coupling force due to hydrodynamic interaction between the OWC pistons motion and the platform.

In addition, both wind and wave power output must be assessed in a hybrid system. However, no coupled simulation tool was available for this work to consider all these couplings. On the one hand, the tool OpenFAST was used, which can consider points 1 and 2, and the wind turbine output power. On the other hand, a Modelica-language-based tool was used in this work, which can consider all four effects and the wave output power, but it is incapable of computing the loads on the wind turbine. A representation of the procedure undertaking is shown in Fig. 1. Sarmiento [21] showed that for the tested conditions, the influence of OWCs on the floating system's dynamics in normal operation is very limited. Therefore, the resulting changes in the wind turbine loads due to points 1 and 2 were analyzed by performing aero-hydro-servo-elastic simulations in OpenFAST. During the design process, if the platform shows increased lifetime DELs in aero-hydro-servo-elastic simulation, the design needs to be iterated. The qualified design is then simulated in the Modelica tool to assess wave energy conversion.

TABLE I
Simulated sea states for wave energy conversion*

SS	T_p [s]	H_s [m]	P [%]	SS	T_p [s]	H_s [m]	P [%]
1	5.00	1.61	1.47	15	12.13	3.95	3.25
2	6.50	5.60	1.21	16	13.40	1.38	2.41
3	7.64	1.26	4.89	17	13.43	2.53	8.40
4	7.60	2.33	4.51	18	13.50	4.04	5.05
5	7.88	3.61	0.09	19	15.25	3.66	1.16
6	11.50	6.38	0.88	20	14.86	1.36	0.89
7	9.04	1.27	10.74	21	14.85	2.53	3.16
8	9.02	2.31	6.46	22	14.88	4.19	3.33
9	9.01	3.75	0.81	23	16.43	1.34	0.25
10	10.51	1.32	9.95	24	16.35	2.47	0.67
11	10.57	2.31	9.35	25	16.30	4.31	0.63
12	10.61	3.96	1.22	26	18.50	3.32	0.37
13	11.96	1.37	6.35	27	18.00	3.37	0.30
14	12.03	2.43	12.19				

*Reduced set of sea states (SS) describing the wave climate at the presented site.

A. Simulated conditions

The simulated conditions were obtained for a site located 35 km off the coast of Portugal in the proximity of Porto, at the coordinates 41°10'27"N 9°03'50"W [22]. The location is situated close to an area that was identified for future offshore wind projects by the Portuguese government. The closest port is the port of Leixões, which is one of the main Portuguese ports. The sea states simulated for the wave energy conversion are shown in Table I. These sea states are a reduced set of sea states derived from the complete wave data at the location from January 1979 to December 2009 by a methodology presented in [23].

B. Aero-hydro-servo-elastic simulation in OpenFAST

OpenFAST is an aero-hydro-servo-elastic time-domain simulation tool developed by NREL for the simulation of horizontal axis wind turbines (HAWTs). It also allows the simulation of floating foundations. In Ref. [24], it is shown that it predicts the essential system effects of floating wind turbines that can be represented by aero-hydro-servo-elastic tools today.

The wind and wave heading were aligned to zero degrees in each simulation case. All simulations were performed for normal turbulent conditions (operational conditions). No extreme events were considered. For each wind speed in the operational wind regime of the wind turbine, the most probable sea states to occur in combination with that wind speed classes were simulated.

C. Base System

The IEA 15 MW offshore reference wind turbine of Class IB is described in Ref. [25] as a monopile bottom-fixed turbine. Ref. [26] adapted the turbine to a floating use case on the VolturnUS-S platform, which is the case

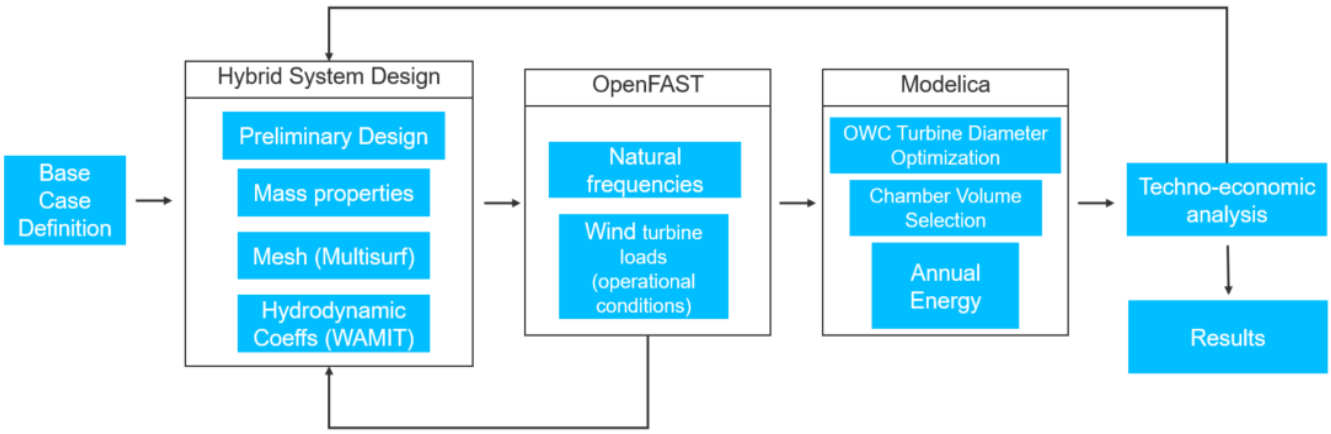

Fig. 1. Methodology followed for the development of the hybrid systems.

considered here. The wind turbine is a conventional 3-bladed variable speed, pitch-regulated HAWT with 15 MW rated power. The rated wind speed is 10.59 m/s with a design tip-speed-ratio of 9.0. Cut-in and cut-out speeds are 3 m/s and 25 m/s, respectively. With a 240 m rotor diameter and a hub height of 150 m it reaches a total height of 270 m and has 30 m clearance below the rotor.

The VolturnUS-S is a semi-submersible floating platform concept developed at the University of Maine. An 11 MW version of it will contribute to the first commercial floating wind project in the United States by 2024 [27]. The 15 MW version VolturnUS-S is a steel version of the platform developed to support the 15 MW reference wind turbine. The floating platform consists of four columns, three radial and one inner column that supports the wind turbine. The columns are connected by three rectangular pontoons located 13m below the sea water level (SWL).

D. Hybrid System Design

The material cost of the ducts is an important cost driver for the hybrid system. The goal of the design, therefore, was to use the material efficiently. The most common solution for semi-submersibles in the literature has the ducts arranged around the columns of the semi-submersible platform, as in Refs. [28] or [18]. This solution is less efficient in terms of material use. The power of the OWCs grows with the area of the duct cross-section. If the platform's column is reducing this area, the WEC will harvest less energy than it could with a duct of this size. Also, the pontoons attached to the bottom of the columns could restrain the motion of the water column and, therefore, may further reduce energy generation. Therefore an alternative approach to placing the ducts independently from the original semi-submersible columns close to the central column of the platform was proposed.

Furthermore, the design of the hybrid platform had two additional constraints:

- The new OWCs' draft should not exceed the draft of the original VolturnUS-S platform.
- The metacentric height shall be kept the same as the original VolturnUS-S original platform.

TABLE II
ADDED MASSES OWC PISTONS

	Piston 1	Piston 2	Piston 3
A^{∞} [kg]	2.719E+06	2.731E+06	2.731E+06

Added masses at infinite frequency for the three OWC pistons. Piston 1 points towards the waves, 2 and 3 are counted counter-clockwise.

Three OWCs were designed to be installed around the central column of the original floating platform. The material of the added-on OWCs ducts was chosen the same as the original platform, steel, and the wall thickness was set to 0.06 m. The duct length was chosen to be the same as the platform draft $\mathrm{DR}_{\mathrm{VolturnUS}}$, which is 20 m. Longer ducts will create issues when handling the platform, so the maximum draft of the new ducts was considered, as aforementioned, a constraint.

The added masses at infinite frequency for the OWCs evaluated for the hybrid design are presented in Table II. A preliminary estimation for the OWC diameter resulted in 18 m. The resonance frequency was estimated using

$$\omega_{\mathrm{nat}} = \sqrt{\frac{\rho g S}{m + A}} \quad , \tag{1}$$

which gives about 10 s resonance period. The approximation with the formula above neglects air compressibility effects and is only valid assuming a linear PTO, and therefore not necessarily transferable to a system using the nonlinear biradial air turbine.

To compensate for the additional weight of the ducts the platform's fluid ballast was reduced. This leads to a higher center of gravity and, therefore, a reduced metacentric height. To obtain the same metacentric height for the platform, anti-heave tanks needed to be attached to the outside of the radial columns, as shown in Fig. 2. The position is beneficial because the horizontal distance from platform CoG to the tanks is large, so that a large increase in moment of inertia, I_{yy}, can be achieved with only a small surface at SWL. The cross-section for the outer shape of the tanks is a semi-circle. The tanks are manufactured from the same steel as the platform, with the same wall thickness, $t_{\mathrm{tanks}} = 0.06\,\mathrm{m}$. The tanks are positioned from a height

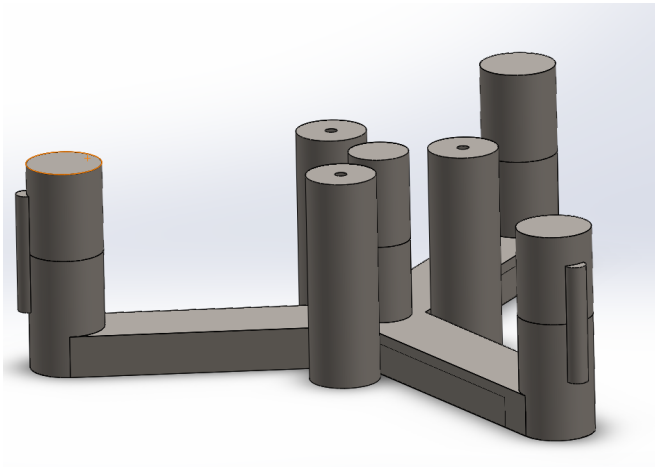

Fig. 2. Hybrid floating platform consisting of the VolturnUS-S floater, three OWC ducts and flotation tanks on the radial columns.

TABLE III
MASS PROPERTIES OF THE DESIGNED HYBRID FLOATING PLATFORM.

	Flotation tanks	OWCs ducts	Hybrid Platform
Mass [$\times 10^3$ kg]	191	1945	18140
CoG [m]	0.00	-1.18	-12.88
Inertia Pitch [kg m^2]	3.397E+08	4.455E+08	1.257E+10
Inertia Yaw [kg m^2]	6.647E+08	4.407E+08	2.335E+10
CoB [m]	-5.00	-10.00	-13.54
Surface area [m^2]	16.95	6.54	470.19
Overall CoG [m]	none	none	0.74
I_{yy} [m^4]	2.92E+04	745.76	5.27E+05
Metacentr. height [m]	none	none	11.43

of -10 m until +10 m relative to the platform reference point (located in a plane at SWL).

E. OWC simulation in Modelica

The model used to simulate the wave-energy conversion of the system was implemented in the open-source modeling language Modelica. The time-domain model is described and validated in Ref. [29]. The system was modeled as a 4-body system, where body 1 is the physical structure and bodies 2 to 4 are the OWCs. These three OWCs were modeled as thin pistons located at the free surface. The equations of motions are as follows

$$\sum_{j=1}^{6}\left(\left(m_{ij}+A_{ij}^{\infty}\right)\ddot{x}_j+R_{ij}+C_{ij}q_j\right)=F_{\mathrm{w,exc},i} +F_{\mathrm{moor},i}+F_{\mathrm{WindTurb},i},\quad i=1,2,4,5,6 \quad , \tag{2}$$

which describes the forces on the platform in all degrees of freedom except for heave (mode 3). DOFs 9, 15, and 21 describe the heave motion of the pistons. Forces on the platform in heave and on the pistons are calculated by

$$\sum_{j=1}^{6}\left(\left(m_{ij}+A_{ij}^{\infty}\right)\ddot{x}_j+R_{ij}+C_{ij}q_j\right)+\left(A_{39}^{\infty}\ddot{x}_9+R_{39}\right) +\left(A_{3,15}^{\infty}\ddot{x}_{15}+R_{3,15}\right)+\left(A_{3,21}^{\infty}\ddot{x}_{21}+R_{3,21}\right)=F_{\mathrm{w,exc},i} +F_{\mathrm{moor},i}+F_{\mathrm{pto},9}+F_{\mathrm{pto},15},+F_{\mathrm{pto},21}\quad i=3 \quad , \tag{3}$$

and

$$\left(m_{99}+A_{99}^{\infty}\right)\ddot{x}_9+R_{99}+C_{99}q_9+A_{93}^{\infty}\ddot{x}_3+R_{93} +A_{9,15}^{\infty}\ddot{x}_{15}+R_{9,15}+A_{9,21}^{\infty}\ddot{x}_{21}+R_{9,21}= F_{\mathrm{w,exc},9}-F_{\mathrm{pto},9} \quad , \tag{4}$$

$$\left(m_{15,15}+A_{15,15}^{\infty}\right)\ddot{x}_{15}+R_{15,15}+C_{15,15}q_{15}+A_{15,3}^{\infty}\ddot{x}_{15} +R_{15,3}+A_{15,9}^{\infty}\ddot{x}_9+R_{15,9}+A_{15,21}^{\infty}\ddot{x}_{21}+R_{15,21}= F_{\mathrm{w,exc},15}-F_{\mathrm{pto},15} \quad , \tag{5}$$

$$\left(m_{21,21}+A_{21,21}^{\infty}\right)\ddot{x}_{21}+R_{21,21}+C_{21,21}q_{21}+A_{21,3}^{\infty}\ddot{x}_{21} +R_{21,3}+A_{21,9}^{\infty}\ddot{x}_9+R_{21,9}+A_{21,15}^{\infty}\ddot{x}_{15}+R_{21,15}= F_{\mathrm{w,exc},21}-F_{\mathrm{pto},21} \quad , \tag{6}$$

respectively. In the equations above, x_j, $\dot{x}_j$, and $\ddot{x}_j$ are the displacement, velocity, and acceleration of the j-th mode. $M_{ij}=m_{ij}+A_{ij}^{\infty}$ terms represent the components of the 24×24 total inertia matrix $\mathbf{M}$, i.e. each M_{ij} component includes the mass and the added mass contributions. Note that the inertia matrix $\mathbf{M}$ is symmetric and comprises many zero values. C_{ij} represents the components of the hydrostatic coefficients matrix $\mathbf{C}$. The terms $F_{\mathrm{k},i}$ are the forces associated with the mooring lines, which in this work were considered linear springs. Also, $F_{\mathrm{WindTurb},i}$ represents the contribution of forces and moments due to the wind turbine, considered mainly in surge and pitch (modes 1 and 5) for the floating platform.

Furthermore, the excitation forces $F_{\mathrm{e},i}$ can be obtained as a sum of N components of frequency ω_n,

$$F_{\mathrm{e},i}(t)=\sum_{n=1}^{N}A_w(\omega_n)\,\Gamma_i(\omega_n)\,\cos\left(\omega_n t+\phi_1+\phi_r\right), \quad i=1,2,...,N\,, \tag{7}$$

where ω_n is the wave frequency of the regular wave component n, $\Gamma_i(\omega_n)$ represents the exciting force or moment response, and $A_w(\omega_n)$ is the incident wave amplitude, both as functions of regular wave component with frequency ω_n. ϕ_r and ϕ_1 are the excitation response phase to the wave component and the phase in the wave generation (a uniform random phase), respectively.

The interaction between pistons and platform is only assumed in the heave direction. The elements R_{ij} describe the wave radiation damping forces, and they are calculated according to

$$R_{ij}=\int_0^t \kappa_{ij}(t-\tau)\dot{x}_j(\tau)d\tau \quad . \tag{8}$$

Instead of direct integration, as in OpenFAST, the radiation impulse response functions κ_{ij} were approximated using Prony's method as presented in Ref. [30].

The compressibility of the air in the OWC air chamber is considered, as presented in Ref. [29]. The air turbine modeled for the OWCs is a biradial air turbine [30].

F. Levelised Cost of Electricity

The levelised cost of electricity can be expressed as

$$\mathrm{LCOE_{wec}} = \frac{\sum_{i=1}^{N} (\mathrm{CAPEX}_i + \mathrm{OPEX}_i + \mathrm{DECEX}_i) \cdot (1+r)^{-i}}{\sum_{i=1}^{N} AEP_i \cdot (1+r)^{-i}} \quad , \tag{9}$$

where CAPEX represents the capital expenditures, assumed concentrated at the beginning of the project; OPEX is the operation and maintenance expenditures, and DECEX is the decommissioning expenditures. Regarding the CAPEX, Martinez [31] reported a LCOE study for large floating wind farms. The study presented CAPEX values for the north coast of Portugal of about 3.5 M€/MW for a floating wind farm of 1 GW of installed capacity. The assumption of a farm of such magnitude and the reported CAPEX are considered in this analysis. The same study reported values of OPEX of 139.4 M€/year applicable to the location under study here (off the coast near Leixões). In Ref. [31], DECEX was reported approximately as 5% of the CAPEX, which was also assumed here. The discount rate r was assumed as 8% [31].

For the base case in this work, i.e. the wind farm without wave energy converters, the LCOE was computed using Eq. 9, and the annual energy yield obtained through the OpenFAST simulations for the joint wave-wind climate of the location, as a function of the wind classes, and their probabilities of occurrences. The base case LCOE was 140 €/MWh for a 1 GW wind farm on the Portuguese coast. This estimation considered an availability factor of 90% and farm losses of 18% [22].

Regarding the hybrid system, the contribution of costs of the WEC and the additional energy yield was accounted for to obtain the corresponding $\mathrm{LCOE_{hyb}}$. The addition of the WECs to the platform is expected not to cause significant additional costs for the floating wind project. Due to the small power generation of the OWC device, no changes in the electric infrastructure are considered. Since the mass of the platform is only marginally increased, and the geometry of the platform only changed slightly, costs for port operations, transport, and platform installation are assumed to remain the same.

The $\mathrm{CAPEX_{wec}}$ for the wave energy converters considers the additional costs due to the materials, fabrication and power take-off system of the WECs. Eq. 10 assumes contributions from turbine cost $\mathrm{C_{turbine}}$, and the steel structure cost $\mathrm{C_{st}}$ that includes all relevant costs for manufacturing these structures from material cost to labor cost and profit of the manufacturer. Labor cost for the turbine are neglected, due to the cost presented was an estimation from a potential manufacturer for the volume of units required.

$$\mathrm{CAPEX_{wec}} = \mathrm{C_{turbine}} + \mathrm{C_{st}} \quad . \tag{10}$$

Base on Myhr [32], the cost of steel considered here is C_{steel} = 1234 €/ton. Furthermore, the manufacturing cost is calculated from the material cost C_{steel} based on a complexity factor. For the WindFloat© semi-submersible, a complexity factor of 200% is given. This value is adopted here for the addition of the ducts to the platform. The cost of structural steel added to the platform can be calculated by Eq. 11

$$\mathrm{C_{st}} = 3 \cdot C_{\mathrm{steel}} \quad . \tag{11}$$

For decommissioning costs, Martinez cites Bjerksetter [33] who concludes for the WindFloat© semi-submersible that for the decommissioning of the platform the return value of scrap steel exceeds the cost of decommissioning by a price of 460 €/ton. Adjusted by inflation, the cost return from decommissioning per ton of structural steel is C_{dec}=-568 €/ton,

$$\mathrm{DECEX_{wec}} = C_{\mathrm{dec}} \cdot m_{\mathrm{steel}} \quad . \tag{12}$$

The OWC's turbine cost is based on a turbine considered for the BlueCAO project [34] from a potential manufacturer. The cost of each biradial air turbine of the selected diameter, described in the next sections, is then considered 498 k€.

The yearly $\mathrm{OPEX_{wec}}$ was considered as a 5% share of the project's $\mathrm{CAPEX_{wec}}$ [35]. The annual energy production of the wave energy converter is calculated from $\bar{P}_{\mathrm{ann,t}}$ by multiplication with the availability factor AF of the OWC device and the duration of one year in hours. The EU-funded OPERA project (Open Sea Operating Experience to Reduce Wave Energy Costs) obtained an availability factor of $AF = 90\%$ for the tested MARMOK-A5 floating OWC device [36], and it is assumed here too,

$$\mathrm{AEP_{wec}} = 8760\, \bar{P}_{\mathrm{ann,t}}\, AF \quad . \tag{13}$$

The final hybrid system $\mathrm{LCOE_{hyb}}$ is computed as a function of the annual energy production of wind $\mathrm{AEP_{wind}}$, the annual energy production of wave $\mathrm{AEP_{wec}}$, and the corresponding costs of electricity of wind and wave, $\mathrm{LCOE_{wind}}$ and $\mathrm{LCOE_{wec}}$, respectively. The equation can be expressed as

$$\mathrm{LCOE_{hyb}} = \frac{\mathrm{LCOE_{wind}\,AEP_{wind}} + \mathrm{LCOE_{wec}\,AEP_{wec}}}{\mathrm{AEP_{wind}} + \mathrm{AEP_{wec}}} \quad . \tag{14}$$

III. RESULTS

A. Aero-Hydro-Servo-Elastic simulations in OpenFAST

In the OpenFAST simulations the power generation of the wind turbine and the damage equivalent loads of the bending moments at the blade roots and tower base were analysed. Fig. 3 and Fig. 4 show the OpenFAST simulation results for the tower base bending moment around the pitch axis. No significant increases in the DELs were observed for the simulated cases. The power generation of the wind turbine

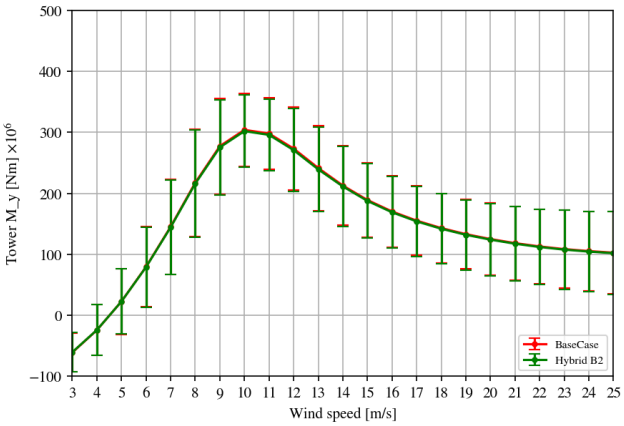

Fig. 3. Mean values and standard deviations for the tower base moments for all windspeeds. Comparison between hybrid platform and base case.

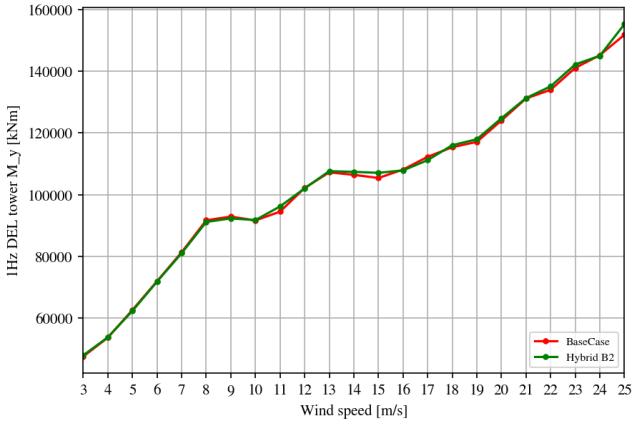

Fig. 4. 1 Hz DELs of the wind turbine tower base moment around pitch-axis for different wind speeds. Comparison between base case and the hybrid device.

was unchanged as well, as deviations for that were below 0.03%. Therefore the hybrid device presented here was seen as qualified for further analysis of the wave energy generation process in the Modelica tool. Nevertheless, it should be noted that the simulations for these results did not consider the coupling forces in the OWC chamber which introduces some degree of uncertainty.

B. Wave Energy Conversion in Modelica

The design selection process requires the simulation of the mean annual power generation for different turbine diameters. The pneumatic power $\bar{P}_{ann,p}$ is the power available to the turbine within the air chamber due to the hydrodynamic response of the oscillating water column motion. The turbine power output $\bar{P}_{\text{ann,t}}$ is lower because of losses in the turbine. The generator was considered ideal (i.e., efficiency equal to 1). Simulation results for $\bar{P}_{ann,p}$ and $\bar{P}_{\text{ann,t}}$ of the hybrid platform are shown in Fig. 5. In these simulations, the air chamber volume was set to $V_{\text{ch}} = 1563\,\text{m}^3$, which corresponds to an air chamber of 15 m height about SWL, as it was assumed in the calculation of mass properties.

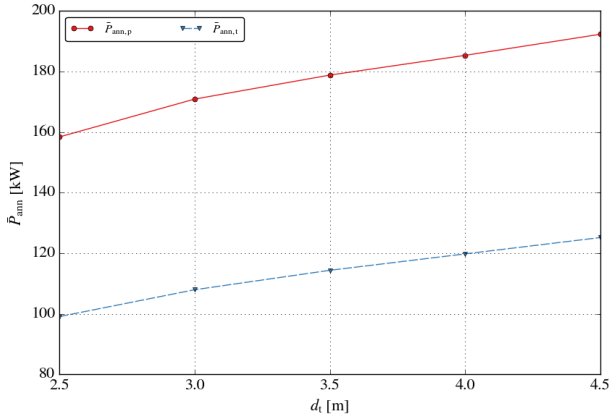

Fig. 5. Mean annual power generation obtained in the Modelica simulations for all sea states for different OWC turbine diameters.

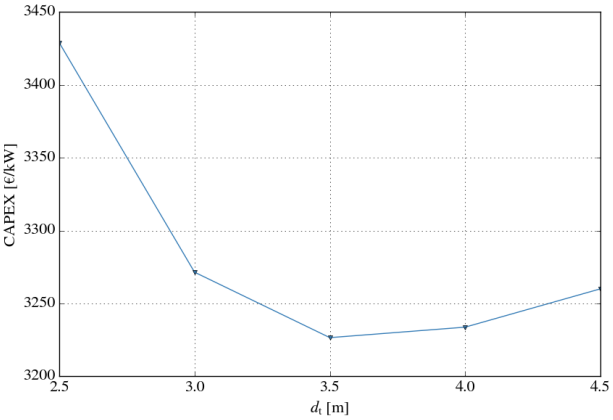

Fig. 6. CAPEX to mean annual power for different OWC turbine diameters obtained by Modelica simulations. The results point at an optimum diameter of 3.5m.

TABLE IV
MEAN ANNUAL POWER GENERATION COMPARISON

Device	$\bar{P}_{\text{ann,t}}$ per unit chamber surface area [kW/m²]
Mutriku [37]	0.78
WindPlat [38]	0.95
Hybrid Platform	0.36

It can be seen that Fig. 5 shows no maximum for $\bar{P}_{\text{ann,t}}$. The maximum occurs for a higher turbine diameter, which would be too large for a real project due to turbine cost. The turbine diameter choice is also a consequence of cost considerations. The influences of the turbine cost and the ducts material cost are summarised in Fig. 10, which shows the ratio of CAPEX to the mean annual generated electric power. As a result, an optimum turbine diameter of $D_{\text{t}} = 3.5\,\text{m}$ is obtained. The mean annual turbine power is $\bar{P}_{\text{ann,t}} = 114\,\text{kW}$.

The obtained power is lower than for other OWC devices. Table IV compares the ratio of mean annual power to the water surface in the OWC chamber of the hybrid device analysed here to values from the literature. These literature values are 2.6 and 2.1 times higher than for the hybrid device investigated here.

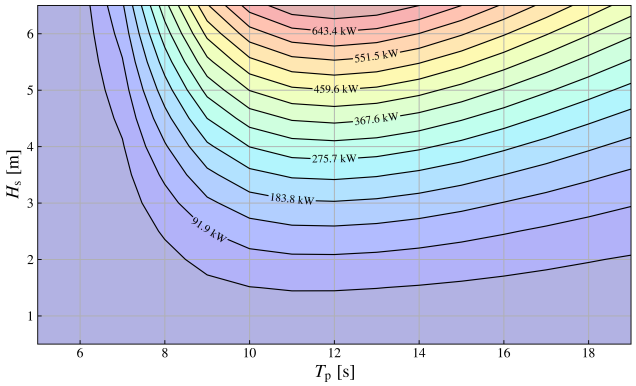

Fig. 7. Turbine power matrix for the hybrid device investigated here with an OWC turbine diameter of 3.5 m.

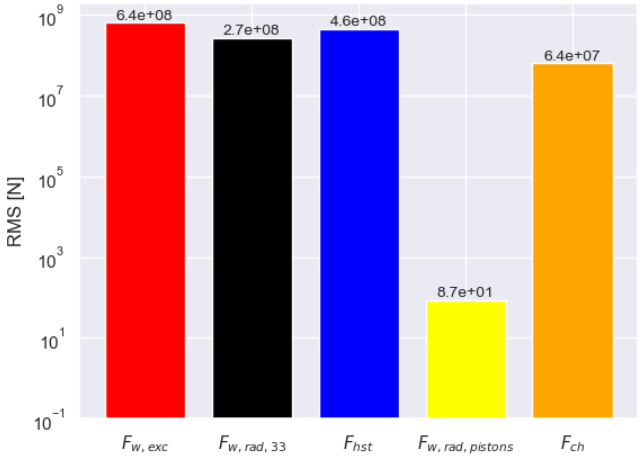

Fig. 8. RMS values of the coupling forces between OWCs including PTO and platform. Coupling due to wave radiation is negligible, but chamber pressure forces have a comparable magnitude to the main hydrodynamic forces.

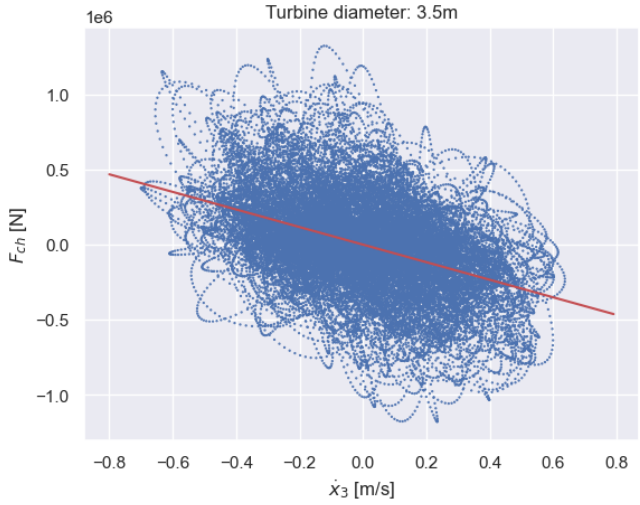

Fig. 9. Chamber pressure forces vs. platform velocity in heave (blue). A weak correlation exists that is approximated by linear regression (red).

Portillo [38], for example, shows the power performance of an OWC can depend on the volume of the air chamber. Other authors have reported similar findings. To investigate if $\bar{P}_{\text{ann,t}}$ depends on the chamber air volume for the selected turbine size, simulations with different chamber volumes were performed for the chosen turbine diameter. Next to the volume that was set for the simulations above, simulations for 60% and 140% of that value were performed. The results did not show significant differences. The conclusion is that the turbine diameter is large enough for the volume not to have a significant influence on the power conversion. Therefore the air chamber height was set to be $H_{\text{ch}} = 15\,\text{m}$, as assumed initially, which corresponds to the freeboard of the VolturnUS-S platform.

Fig. 7 shows the power matrix of the designed wave energy converters. The simulations were done in the time domain, using the Modelica tool being developed at IST/ULisboa, for 4000 s, and the last 3600 s were considered for the analysis. The highest power is generated for sea states with $T_p \approx 12\,\text{s}$. This is especially the case for sea states with large H_s. About 59% of the annual energy for the investigated sea states (see Table I) is contained in sea states with peak periods between 12-15 s. About 33% are present in periods below that range. So the OWCs period of maximum energy generation is already well positioned, in proximity to the sea states of highest annual energy, but also generating considerable energy for sea states with lower T_p. Future work will consider changes in the ducts' characteristics, as a potential strategy to increase mean annual power output $\bar{P}_{\text{ann,t}}$. This might be achieved by enlarging the cross section areas of the OWCs, despite of the inherent change of the resonance period.

C. Coupling Forces in Modelica

The simulations performed in OpenFAST to determine changes in wind turbine loads are not considering any influences on the platform dynamics that the WEC PTO might have. To assess the influence of these interactions the coupling forces due to OWC air chamber pressure and wave radiation force are analyzed here. Furthermore, a modeling approach for these forces is presented that would allow the inclusion of PTO effects into aero-hydro-servo-elastic simulations in OpenFAST.

Wave excitation force, wave radiation force, and hydrostatic forces on the floater are all calculated separately in Modelica. The hydrodynamic coupling forces between the pistons and the platform due to radiation are calculated as well. Furthermore, from the pressure time series, the force on the platform due to OWC chamber pressure can be calculated as

$$F_{\text{ch},1} = S_{\text{ch}}\, p_{\text{ch},1}(t) \quad . \tag{15}$$

The following considerations were performed for the sea state, which has the highest contribution to the annual energy yield of the OWCs with a significant wave height of $H_s = 2.43\,\text{m}$ and a peak period of $T_p = 12.03\,\text{s}$. Only the forces in heave motion are considered here. The RMS values of the considered forces are shown in Fig. 8, where the values for wave radiation coupling and chamber pressure force consider the sum of forces of all three pistons. It can be seen that the platform forces due to wave radiation of the pistons $F_{\text{w,rad,pistons}}$ are negligible compared to the

other forces acting on the platform. This means that the aero-hydro-servo-elastic simulations in OpenFAST approximate a simulation with an open air chamber of the OWCs (i.e. without force due to chamber pressure) very well.

Even though smaller in this case, the forces due to chamber pressure F_{ch} have a similar order of magnitude as the hydrodynamic forces already considered in OpenFAST. That means the aero-hydro-servo-elastic simulations in OpenFAST neglect a significant physical effect. The results obtained in this way may, therefore, not be transferrable to an operational device that is using an air turbine and generates electricity since the additional forces may alter platform motion and, subsequently, turbine loads.

As explained above, OpenFAST has no capabilities to model the OWCs directly. However, it is possible to include additional force terms depending on the platform position or velocity. This can be done by matrices for linear stiffness, linear damping, and quadratic damping. In order to properly model the OWC forces they must fulfill a relationship in the form $F_{\text{ch}} = f(x_3)$ and/or $F_{\text{ch}} = f(\dot{x}_3)$.

The chamber forces are plotted against the platform heave velocity in Fig. 9. A moderate correlation can be observed. A linear approximation of the OWC chamber forces is presented in Eq. 16. The resulting damping for the linear damping matrix when including this term in OpenFAST is positive, which suggests that, on average, the OWCs are damping the platform motions for the case analyzed here.

$$F_{\text{ch}}^{\text{model}} = -585 \frac{\text{kNs}}{\text{m}} \dot{x}_3 \tag{16}$$

The mean absolute estimation error for all plotted points is $220\,\text{kN}$, the maximum error is 1108 kN, which is large considering the maximum predicted force by the model is 410 kN. The RMS of the modeled force $F_{\text{ch}}^{\text{model}}(t)$ (2.7×10^7 N) is smaller than the value for the estimation error (5.8×10^7 N). These results show that modeling the forces related to the PTO in OpenFAST using the linear damping matrices may not deliver accurate results.

D. LCOE results

Table V presents the main cost components, the wave-rated power, and the annual energy yield of the wave power system for one platform. Table VI presents the results of the LCOE for the wave energy conversion system designed as add-on features and the LCOE of the hybrid platform for discounts rates of 8% and 10% and project lifetimes of 20 and 25 years.

The resulting LCOE for the wave energy generated by a farm of 67 floating hybrid wind-wave systems is $\text{LCOE}_{\text{wec}} = 1485 \frac{€}{\text{MWh}}$ for a discount rate of 8% and $\text{LCOE}_{\text{wec}} = 1662 \frac{€}{\text{MWh}}$ for a discount rate of 10%, both estimated for a project lifetime of 25 years. This is significantly larger than the values for floating wind presented in Ref. [31]. It should be evident that to reduce the hybrid's system cost of energy, the wave energy conversion system's cost of energy shall be lower than the wind energy's. In the WEC design presented, the wave energy system has a much smaller power generation than the wind energy system. In addition, the high CAPEX of the steel cylinders for the OWCs and the PTO costs contribute to the high LCOE_{wec}. The additional lifetime cost due to the WEC and its cost contributions is presented in Fig. 10. The CAPEX expenses contribute the majority of the costs with 66%, and OPEX contributes 33%. In the CAPEX the material and manufacturing costs for the ducts contribute the dominant share. This emphasises the importance of conceiving solutions with alternative non-metallic materials, maybe concrete-based solutions for the add-on features. It should be highlighted again that since the manufacturing cost here is calculated from the ducts material cost the steel sheet thickness also influences the manufacturing costs.

The LCOE obtained here is higher than the LCOE values usually cited for wave energy. For example, Ref. [39] gives an LCOE of $100 - 400 \frac{€}{\text{MWh}}$. Differences might be explained by: i) the high CAPEX cost shown above, which also determines the OPEX for the analysis here; ii) the fact that the design conceived in this work is an add-on to an existing platform, which limits the optimisation of the wave energy system; and iii) the use of biradial air turbines for the WEC system, which are relatively efficient, but potentially costlier than other types of air turbines for OWCs. Furthermore, for the specific design here, an important factor determining the cost is the wall thickness of the OWC ducts. This parameter was only roughly estimated for the analysis here and therefore introduces a large uncertainty in the cost estimations. Another reason is the low energy generation of the device. It should be mentioned that no optimization of the OWC duct geometry was performed for the OWC design. A different choice for the diameter and shape of the ducts might result in increased power generation.

TABLE V
CAPEX, OPEX AND DECEX COMPONENTS FOR THE THREE OWCS AS ADD-ON FEATURES FOR ONE HYBRID FLOATING PLATFORM. ALSO, RATED WAVE POWER FOR THE SET OF THREE OWCS AND AEP IN THE LOCATION OF STUDY.

Variable	Value	Unit
Steel structure mass (due to OWCs)	2136	$\times 10^3$ kg
Steel material cost (due to OWCs)	2635824	€
Steel structure labor cost (due to OWCs)	5271648	€
OWC air turbine diameter	3.5	m
OWC air turbines' cost (x3)	1496133	€
$\text{CAPEX}_{\text{wec}}$	9403605	€
OPEX_{wec} yearly	470180	€
$\text{DECEX}_{\text{wec}}$ undiscounted	-1213248	€
Wave rated power per platform	450	kW
AEP	900	MWh

The use of the hybrid platform conceived for this work does not decrease the LCOE of the reference floating wind project. The hybrid system's levelised cost of electricity is $\text{LCOE}_{\text{hyb}} = 147 \frac{€}{\text{MWh}}$ and $\text{LCOE}_{\text{hyb}} = 164 \frac{€}{\text{MWh}}$ for 8% and 10% discount rates, respectively, considering a project lifetime of 25 years. The increase in overall LCOE is due mainly to the high CAPEX and the low annual energy yield of the WEC systems.

TABLE VI
RESULTS OF THE LCOE CALCULATION FOR THE WAVE ENERGY CONVERSION SYSTEMS AND HYBRID SYSTEMS IN A FARM, AS PRESENTED IN REF. [31].

Variable	20 y r=8%	25 y r=8%	20 y r=10%	25 y r=10%
$LCOE_{wec}$ [€/MWh]	1559	1485	1729	1662
$LCOE_{hyb}$ [€/MWh]	156	147	173	164

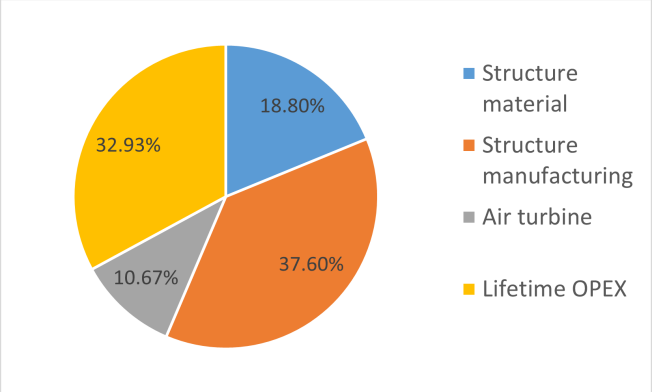

Fig. 10. Lifetime cost contributions for the wave energy converter.

IV. CONCLUSIONS

This work aimed to design wave energy systems of the oscillating water column type as add-on features to an existing wind floating platform. The work demonstrated that the design of these add-ons is feasible, but the power output of the wave conversion systems and the high capital expenditures have a negative impact on the levelised cost of electricity of the hybrid system.

Aero-hydro-servo-elastic simulations under irregular waves and turbulent wind fields were performed in OpenFAST for the designed hybrid floating platform without considering the coupling between the floater and the OWC pistons. The aim was to analyze the potential negative effects on the wind turbine in terms of loads and power production. Furthermore, the wave energy power generation was estimated through the OWC Modelica tool. This was followed by a selection process of a biradial air turbine and air volume for the OWCs. From the Modelica simulation results, the influence of the OWC's PTO was identified as non-negligible. This means the aero-hydro-servo-elastic simulations performed in OpenFAST neglect an important effect. Therefore, it could be that the observations connected to wind turbine damaged equivalent loads, which in the current work were practically not altered with the addition of the wave energy systems, do not hold true when the full coupling is considered. Possible approaches for including these effects in OpenFAST simulations were assessed.

The investigation in this work was only performed for operational conditions. Influences of the additional OWCs on the platform behavior and turbine design loads in extreme conditions were not assessed. The hybrid systems investigated here might have positive or negative consequences for platform stability in extreme conditions that were not observable in this analysis.

The mean annual wave power generation of 114 kW in the location selected obtained for the device is significantly smaller than what would be expected for a device of this size comparing it to other OWC devices. The resulting LCOE for the OWC alone is by a factor of 10 higher than the LCOE of the floating wind platform alone. In projects of smaller scope, i.e. for niche applications with lower power level requirements, the floating wind LCOE may be larger, and the gap to the wave energy converter's LCOE may be smaller. Additional benefits are present for autonomous grids that can also profit from the lower power output variability of the wave energy converters. In the literature review, it was shown that wind-wave hybrid systems might have other beneficial effects than a possible LCOE reduction that were not considered in this work [6]. The WEC could dampen the overall motion of the platform and therefore reduce damage equivalent loads on the wind turbine.

Multiple approaches can be followed to improve the results for the OWC's performance and LCOE. Increasing the duct diameter may increase AEP, and so may an advanced control scheme like latching [20]. Another approach is to reduce CAPEX, maybe the use of concrete-based solutions for the OWCs and smaller (cheaper) air turbines in higher numbers per OWC.

Furthermore, more investigation should be done for other types of OWC WEC designs, which have been proven more efficient and have larger power outputs. Future work will consider the use of new capabilities of Hydrodyn, used with OpenFAST, to model various hydrodynamic potential flow bodies and the inclusion of external forces, as those encountered in the air chamber of the OWCs, and the optimisation of floating platforms with different kinds of OWCs.

REFERENCES

[1] European Commission, "The European Green Deal," 2022. [Online]. Available: https://eur-lex.europa.eu/legal-content/EN/TXT/?uri=CELEX:52019DC0640
[2] EC, "Boosting offshore renewable energy for a climate neutral Europe," 2020. [Online]. Available: https://ec.europa.eu/commission/presscorner/detail/en/ip_20_2096
[3] DNV, "Floating wind: The power to commercialize: Insights and reasons for confidence," 2020. [Online]. Available: https://www.dnv.com/focus-areas/floating-offshore-wind/commercialize-floating-wind-report.html
[4] IRENA, "Innovation outlook ocean energy technologies," 2020. [Online]. Available: https://www.irena.org/publications/2020/Dec/Innovation-Outlook-Ocean-Energy-Technologies
[5] J. Cruz and M. Atcheson, Eds., *Floating offshore wind energy: The next generation of wind energy*, ser. Green energy and technology. Switzerland: Springer, 2016.
[6] C. Pérez-Collazo, D. Greaves, and G. Iglesias, "A review of combined wave and offshore wind energy," *Renewable and Sustainable Energy Reviews*, vol. 42, pp. 141–153, 2015.
[7] C. Kalogeri, G. Galanis, C. Spyrou, D. Diamantis, F. Baladima, M. Koukoula, and G. Kallos, "Assessing the european offshore wind and wave energy resource for combined exploitation," *Renewable Energy*, vol. 101, pp. 244–264, 2017.
[8] E. Petracca, E. Faraggiana, A. Ghigo, M. Sirigu, G. Bracco, and G. Mattiazzo, "Design and techno-economic analysis of a novel hybrid offshore wind and wave energy system," *Energies*, vol. 15, no. 8, p. 2739, 2022.
[9] Z. Chen, J. Yu, J. Sun, M. Tan, S. Yang, Y. Ying, P. Qian, D. Zhang, and Y. Si, "Load reduction of semi-submersible floating wind turbines by integrating heaving-type wave energy converters with bang-bang control," *Frontiers in Energy Research*, vol. 10, 2022.

[10] A. Aubault, M. Alves, A. Sarmento, D. Roddier, and A. Peiffer, "Modeling of an oscillating water column on the floating foundation windfloat," in *Proceedings of the ASME 2011 30th International Conference on Ocean, Offshore and Arctic Engineering. Volume 5: Ocean Space Utilization; Ocean Renewable Energy. Rotterdam, The Netherlands. June 19–24, 2011. pp. 235-246. ASME.*, vol. 5, 2011. [Online]. Available: https://doi.org/10.1115/OMAE2011-49014

[11] P. Aboutalebi, F. M'zoughi, I. Garrido, and A. Garrido, "Performance analysis on the use of oscillating water column in barge-based floating offshore wind turbines," *Mathematics*, vol. 9, p. 475, 02 2021.

[12] A. Abazari, "Dynamic response of a combined spar-type FOWT and OWC-WEC by a simplified approach," *Renewable Energy Research and Applications*, vol. 4, pp. 66–77, 2023.

[13] J. M. Kluger, *Synergistic Design of a Combined Floating Wind Turbine - Wave Energy Converter*. MIT Press, 2017.

[14] Y. Zhou, D. Ning, W. Shi, L. Johanning, and D. Liang, "Hydrodynamic investigation on an OWC wave energy converter integrated into an offshore wind turbine monopile," *Coastal Engineering*, vol. 162, p. 103731, 2020.

[15] Floating Power Plant, "The FPP Platform." [Online]. Available: https://www.floatingpowerplant.com/products/

[16] Marine Power Systems, "Pelagen - advanced wave energy converter." [Online]. Available: https://www.marinepowersystems.co.uk/pelagen/

[17] E. Quevedo, "Modular multi-purpose offshore platforms, the TROPOS project approach," 2012. [Online]. Available: https://www.wavec.org/contents/files/sessao-iii-4-eduardo-quevedo.pdf

[18] D. Zhang, Z. Chen, X. Liu, J. Sun, H. Yu, W. Zeng, Y. Ying, Y. Sun, L. Cui, S. Yang, P. Qian, and Y. Si, "A coupled numerical framework for hybrid floating offshore wind turbine and oscillating water column wave energy converters," *Energy Conversion and Management*, vol. 267, p. 115933, 2022.

[19] M. Sojo and G. Auer, "Marine renewable integrated application platform: Final summary report," 2014. [Online]. Available: https://cordis.europa.eu/project/id/241402/reporting

[20] A. F. O. Falcão and J. C. C. Henriques, "Oscillating-water-column wave energy converters and air turbines: A review," *Renewable Energy*, vol. 85, pp. 1391–1424, 2016.

[21] J. Sarmiento, A. Iturrioz, V. Ayllón, R. Guanche, and I. J. Losada, "Experimental modelling of a multi-use floating platform for wave and wind energy harvesting," *Ocean Engineering*, vol. 173, pp. 761–773, 2019.

[22] J. G. Strag, "Offshore floating wind farms cost reduction assessment. Thesis to obtain the Master of Science Degree in Energy Engineering and Management. Instituto Superior Técnico, University of Lisbon," 2022.

[23] R. P. F. Gomes, J. C. C. Henriques, L. M. C. Gato, and A. F. O. Falcão, "Hydrodynamic optimization of an axisymmetric floating oscillating water column for wave energy conversion," *Renewable Energy*, vol. 44, pp. 328–339, 2012.

[24] A. N. Robertson, F. Wendt, J. M. Jonkman, W. Popko, H. Dagher, S. Gueydon, J. Qvist, F. Vittori, J. Azcona, E. Uzunoglu, C. G. Soares, R. Harries, A. Yde, C. Galinos, K. Hermans, J. B. de Vaal, P. Bozonnet, L. Bouy, I. Bayati, R. Bergua, J. Galvan, I. Mendikoa, C. B. Sanchez, H. Shin, S. Oh, C. Molins, and Y. Debruyne, "OC5 Project Phase II: Validation of Global Loads of the DeepCwind Floating Semisubmersible Wind Turbine," *Energy Procedia*, vol. 137, pp. 38–57, 2017.

[25] E. Gaertner, J. Rinker, L. Sethuraman, F. Zahle, B. Anderson, G. Barter, N. Abbas, F. Meng, P. Bortolotti, W. Skrzypinski, G. Scott, R. Feil, H. Bredmose, K. Dykes, M. Shields, C. Allen, and A. Viselli, "Definition of the IEA Wind 15-Megawatt Offshore Reference Wind Turbine," 2020. [Online]. Available: https://www.osti.gov/biblio/1603478

[26] C. Allen and A. Viselli, "Definition of the UMaine VolturnUS-S Reference Platform Developed for the IEA Wind 15-Megawatt Offshore Reference Wind Turbine. Technical Report." 2020. [Online]. Available: https://www.nrel.gov/docs/fy20osti/76773.pdf

[27] University of Maine, "VolturnUS." [Online]. Available: https://composites.umaine.edu/volturnus/

[28] Principle Power, "WindWaveFloat (WWF): Final Scientific Report," 2010. [Online]. Available: https://www.osti.gov/biblio/1057931

[29] J. C. C. Portillo, L. M. C. Gato, J. C. C. Henriques, and A. F. O. Falcão, "Implications of spring-like air compressibility effects in floating coaxial-duct OWCs: Experimental and numerical investigation," *Renewable Energy*, vol. 212, pp. 478–491, 2023.

[30] J. C. C. Henriques, J. C. C. Portillo, W. Sheng, L. M. C. Gato, and A. F. O. Falcão, "Dynamics and control of air turbines in oscillating-water-column wave energy converters: Analyses and case study," *Renewable and Sustainable Energy Reviews*, vol. 112, pp. 571–589, 2019.

[31] A. Martinez and G. Iglesias, "Mapping of the levelised cost of energy for floating offshore wind in the European Atlantic," *Renewable and Sustainable Energy Reviews*, vol. 154, p. 111889, 2022.

[32] A. Myhr, C. Bjerkseter, A. Ågotnes, and T. A. Nygaard, "Levelised cost of energy for offshore floating wind turbines in a life cycle perspective," *Renewable Energy*, vol. 66, pp. 714–728, 2014.

[33] C. Bjerksetter and A. Agotnes, "Levelised costs of energy for offshore floating wind turbine concepts." [Online]. Available: https://nmbu.brage.unit.no/nmbu-xmlui/handle/11250/189073

[34] WavEC, "Bluecao." [Online]. Available: https://www.wavec.org/en/research-development/projects/bluecao

[35] T. Bloise Thomaz, D. Crooks, E. Medina-Lopez, L. van Velzen, H. Jeffrey, J. Lopez Mendia, R. Rodriguez Arias, and P. Ruiz Minguela, "O&M models for ocean energy converters: Calibrating through real sea data," *Energies*, vol. 12, no. 13, p. 2475, 2019.

[36] TECNALIA, "Floating OWC control algorithms: Deliverable D4.3: Opera Project. Technical Report, 2019." [Online]. Available: http://opera-h2020.eu/wp-content/uploads/2019/09/OPERA_D4.3_Floating-OWC-control-algorithms_TECNALIA_20190730_v1.1.pdf

[37] Y. Torre-Enciso, I. Ortubia, L. I. López de Aguileta, and J. Marqués, "Mutriku Wave Power Plant: from the thinking out to the reality," in *Proceedings of the 8th European Wave and Tidal Energy Conference*, Uppsala, Sweden, 2009.

[38] J. C. C. Portillo, "Oscillating-water-column systems: single devices, arrays and multi-purpose platforms." PhD Thesis. Instituto Superior Técnico, University of Lisbon, 2022.

[39] B. Guo and J. V. Ringwood, "A review of wave energy technology from a research and commercial perspective," *IET Renewable Power Generation*, vol. 15, no. 14, pp. 3065–3090, 2021.